

Identification of Core Predication-Related Candidate Genes in Ovarian Cancer Based on Integrated Bioinformatics and Experiment

Jiaqing Bi

Shanxi Medical University <https://orcid.org/0000-0003-0440-9025>

Qian Qin

Shanxi Medical University

Huihan Ma

Shanxi Medical University

Meijie Ma

Shanxi Medical University

Qinmei Feng (✉ qinmei_feng@163.com)

Shanxi Medical University

Research

Keywords: TTK, bioinformatics, Epithelial ovarian cancer, Immunohistochemistry, prediction

Posted Date: August 3rd, 2021

DOI: <https://doi.org/10.21203/rs.3.rs-757589/v1>

License:  This work is licensed under a Creative Commons Attribution 4.0 International License.

[Read Full License](#)

Abstract

Background: Ovarian cancer is one of the deadliest and most common gynecological malignancies. This study aims to use comprehensive bioinformatics analysis to try to identify the core candidate genes related to the prediction of ovarian cancer for the early diagnosis and prognosis of ovarian cancer.

Methods: Obtain expression profiles from Gene Expression Omnibus database, identify differentially expressed genes (DEG) with $p < 0.05$ and $(\log FC) > 1.5$, perform functional enrichment, protein-protein interaction (PPI) network construction, functional module analysis, and survival analysis And correlation analysis to obtain the target gene, through immunohistochemical staining, clinicopathological feature analysis to verify the expression and clinical significance of TTK.

Results: 1. Identified 135 genes with the same expression. 33 up-regulated DEG were mainly enriched in mitotic spindle assembly checkpoints, chromosome segregation regulation, etc.; 102 down-regulated DEG was mainly enriched in neurotransmitter level regulation, protein serine/threonine Regulation of acid kinase activity, etc. Then the PPI network was constructed to screen 20 hub genes and perform survival analysis and expression correlation analysis. At the same time, the modules that met the requirements were screened and the genes were analyzed by pathway enrichment. It was found that TTK was highly expressed in ovarian cancer and led to a poor prognosis. 2. Distant metastasis, lymph node metastasis, clinical staging (stage III-IV), and poor differentiation are independent risk factors for high TTK expression ($P < 0.05$). 3. TTK, CA125, HE4 three biological indicators show excellent diagnostic value in joint monitoring of ovarian cancer.

Conclusions: TTK plays a vital role in the tumorigenesis, aggressiveness and malignant biological behavior of EOC, and can be used as a potential biomarker and potential therapeutic target for early diagnosis and predictive evaluation of EOC.

Introduction

Ovarian cancer is one of the most common gynecological malignancies in the female reproductive system worldwide, with the characteristics of high metastasis, chemotherapy resistance, and postoperative recurrence (1,2). The 5-year survival rate of early (I, II) ovarian cancer is about 90%, while only 20–40% of patients with advanced (III, IV) ovarian cancer have a survival time of more than 5 years (3, 4). More than 70% of patients are at an advanced stage at the time of diagnosis, and the morbidity and mortality of OC patients have increased significantly in recent years. Despite advances in treatment, the 5-year survival rate of OC patients is still less than 40% (5). Epithelial ovarian cancer (EOC) has the highest mortality rate among gynecological malignancies, and it is still the deadliest type that threatens the life and health of women (6). Despite some understanding of it, treatment and survival trends have not changed significantly because early diagnosis remains a challenge. This is partly due to several factors; lack of clear screening tools, vague signs and symptoms may be "disguised" as other non-malignant diseases (7).

Given the lack of specific diagnostic and prognostic molecular markers for EOC, many studies have confirmed the effectiveness of serum human epididymis secretory protein 4 (HE4) in the preoperative diagnosis of patients with ovarian tumors. Verify its specificity. The sensitivity of HE4 and carbohydrate antigen 125 (CA125) overlapped (79%) and HE4 showed a significantly higher specificity than CA125 (93% vs. 78%). They also confirmed that HE4 is superior to CA125 in the diagnosis of ovarian cancer. Although HE4 has higher sensitivity and specificity than CA125 in the diagnosis stage, the combination of the two markers seems to be beneficial (8). Nevertheless, a single indicator used to evaluate EOC is greatly affected by individual differences, so finding new indicators and combining them with existing indicators to predict the development and outcome of EOC has important clinical significance. Besides, gene dysregulation has been shown to play a key role in the occurrence of EOC (7). In the era of targeted therapy, mutation analysis of cancer is a key aspect of making treatment decisions. Therefore, looking for a sensitive and specific biomarker for early diagnosis and predictive evaluation of EOC, and becoming a target for ovarian cancer treatment is vital. Currently, bioinformatics analysis methods are often used in research to identify potential biomarkers that affect disease development.

In this study, we downloaded four original microarray data sets (GSE54388, GSE27651, GSE18520, and GSE26712) from the NCBI Gene Expression Comprehensive Database, with a total of 329 samples, including 297 epithelial ovarian cancer samples and 32 normal ovarian samples. Use R software to identify differentially expressed genes (DEG) between epithelial ovarian cancer and normal controls, and perform functional enrichment analysis. Also, a PPI network of 135 DEGs and key modules was established, and module analysis, survival analysis, and correlation analysis were performed. Through literature review, the important gene TTK related to epithelial ovarian cancer prediction was finally obtained.

Threonine and tyrosine kinase (TTK) is a dual-specific protein kinase that can phosphorylate threonine/serine and tyrosine (9). It is the core component and main regulator of the spindle assembly checkpoint (SAC), which can recruit and coordinate other SAC protein kinases to the kinetochore, thereby ensuring faithful chromosome separation and maintaining genome stability (10,11). Elevated levels of TTK are easily found in many types of human tumors, such as glioblastoma, thyroid cancer, breast cancer, hepatocellular carcinoma, pancreatic cancer, and prostate cancer (12–18). This differential expression is suggested that can be used as a molecular biomarker for clinical diagnosis. We reviewed relevant clinical studies and trials on TTK in several human cancers (19), however, no experimental studies on TTK expression in EOC patients were found. In this study, we used immunohistochemistry to detect the expression of TTK in ovarian epithelial tumor specimens and analyzed the relationship between TTK expression and clinicopathological parameters of EOC patients.

Conclusion

gene expression profile data. This study included four GEO data sets, including a total of 297 ovarian cancer samples and 32 healthy control samples (Table 2). They were standardized by the limma software package in the R/Bioconductor software (Fig. 1). 812, 2820, 1495 and 536 DEGs were screened out

respectively ($P < 0.05$, $|\log_{2}FC| > 1.5$). The differentially expressed genes in the sample data of the 4 data sets are shown in Fig. 2 (Fig. 2). Use VennDiagram package to perform gene integration of DEG that meets the standard. In conclusion, compared with normal OV tissue, a total of 135 (33 up-regulated genes and 102 down-regulated genes) in OC tissue samples were identified as DEG (Table 3).

enrichment analysis. The cluster profiler package was used in R software to biologically annotate 33 up-regulated DEGs and 102 down-regulated DEGs after integration, and the GO function enrichment with P -value < 0.05 was obtained. The significant results of GO enrichment analysis showed that: 1. In the cell composition, the up-regulated DEG is mainly enriched in the double-strain tight junction, late promotion complex, apical junction complex, tight junction, and nuclear ubiquitin junction complex. Down-regulated DEG is mainly enriched in the extracellular matrix, collagen-containing extracellular matrix, and blood particles; 2. In biological processes, up-regulated DEG is enriched in mitotic spindle assembly checkpoints, chromosome separation and regulation, and cell cycle The regulation of later transitions, the positive regulation of ubiquitin-protein ligase activity, the involvement of signal transduction in gene expression regulation and chromosome separation, etc. The down-regulated DEG is obviously enriched in the regulation of neurotransmitter levels, the regulation of blood coagulation, protein serine/threonine The regulation of amino acid kinase activity, the process of mucopolysaccharide metabolism, and the Wnt signaling pathway; 3. In the molecular function group, the down-regulated DEG is mainly enriched in heparin-binding and frizzled binding, while the up-regulated DEG is not significantly enriched in compliance with the standard. (Table 4 & Fig. 3)

PPI network and module analysis. The STRING database was used to establish a PPI network, and 152 protein pairs were obtained. The PPI network was constructed after the comprehensive score > 0.4 and the removal of 29 individual nodes (Fig. 4). The gene data was input into Cytoscape software, and a PPI network diagram containing 29 up-regulated DEG and 77 down-regulated DEG was further obtained. MCODE detected a total of 4 modules, and we chose the module with a higher score for the next analysis (Fig. 5). Use the MCC algorithm in Cytohubba to get the top 20 hub genes, which are: KDR, SOX9, EPCAM, WNT5A, FGF13, PDGFRA, CP, ALDH1A1, KLF4, CDC20, UBE2C, FGF9, SOX17, TTK, TRIP13, CKS2, RACGAP1, CD24, CHGB, LAMB1.

gene enrichment through KEGG pathway. In order to understand the functions of the modules, we have performed KEGG enrichment analysis for each module. The results are shown in (Table 5). TRIP13, RACGAP1, CKS2, UBE2C, TTK, and CDC20 in module 1 all up-regulate DEG, which is mainly enriched in the cell cycle and ubiquitin-mediated proteolysis pathways. There are four genes ALDH1A1, CD24, EPCAM, and SOX9 in module 2. Except for ALDH1A1 which is down-regulated DEG, the other 3 genes are all up-regulated DEG. There is no obvious pathway enrichment in this module. There are four genes CP, LAMB1, CHRDL1, and CHGB in module 3. Except for CP which up-regulates DEG, the rest are down-regulated DEG. After enrichment, CP exists in iron death, porphyrin, and chlorophyll metabolism pathways, and LAMB1 is in ECM receptor Interaction, small cell lung cancer, and other pathways exist.

*survival analysis and expression level analysis of hub gene.*We used the Kaplan Meier Plotter online website to analyze the survival of 20 hub genes and found that 13 genes associated with ovarian cancer have a poor prognosis ($P < 0.05$, Fig. 6). Then use the GEPIA online database to mine the expression levels of 13 genes between ovarian cancer patients and normal people. The results showed that compared with normal ovarian samples, among the 13 prognostic-related genes in ovarian cancer samples, SOX9, EPCAM, CP, UBE2C, TTK, RACGAP1, and CD24 7 genes reflected high expression ($P < 0.01$, Fig. 7).

*clinicopathological characteristics and TTK expression.*In this study, the average age of all patients at surgery was 52 years, and the median age was 53 years. Among them, 59.1% of patients with epithelial ovarian cancer have lymph node metastasis. The proportion of middle-high-middle-differentiated cancer was 43.0%. 56.9% of patients had distant metastases. We found that the expression of TTK was negative in normal ovarian tissues. In tumor tissues, all specimens had positive cytoplasmic staining, and the expression of a benign group, borderline group, and malignant group increased in turn. We calculated the H score of TTK expression in tumor tissues. Among them, the H score is 180 (10–220).(Table 6&Figure 8)

*analysis of the correlation between TTK expression and clinicopathological factors.*We found that there was no significant correlation between TTK expression and age and fertility level. However, there is a significant positive correlation between TTK expression and tumor differentiation, CA125 level, HE4 level, clinical stage, lymphatic metastasis, and distant metastasis. Compared with patients with normal CA125, HE4, moderately well-differentiated, stage I-II, no lymph node metastasis, and no distant metastasis, CA125 elevated, HE4 elevated, poorly differentiated, stage III-IV, lymph node metastasis, and distant metastasis patients, TTK expression rate is higher, multivariate logistic regression analysis with statistically significant clinical-pathological factors in the univariate analysis as independent variables, the results show: distant metastasis, lymph node metastasis, clinical stage (III-IV), Poor differentiation is an independent risk factor for high TTK expression ($P < 0.05$).(Table 7&Table 8)

the ROC curve analysis of TTK, CA125, and HE4 alone and combined detection for diagnosis of ovarian cancer. Draw the ROC curve with the benign ovarian tumor group as the reference, and calculate the AUC, the AUC of TTK, CA125, and HE4 in the joint monitoring of ovarian cancer are 0.927, 0.899, and 0.882, respectively, which are significantly higher than when each index is tested separately. The three biological indicators of TTK, CA125, and HE4 show excellent diagnostic value in the joint monitoring of ovarian cancer.(Fig. 9)

Discussion

Genetic instability is a hallmark of cancer cells. This instability is caused by aneuploidy, with an abnormal genome structure and an abnormal number of chromosomes. This state is closely related to chromosome instability (CIN) (34). SAC is a key monitoring mechanism. It prevents the misdivision of chromosomes by delaying the process of mitosis until all chromosomes are correctly attached to the spindle microtubules, which can ensure the accurate separation of chromosomes. The inactivation of the spindle assembly checkpoint will lead to the premature exit of the mitotic point, which will eventually lead to chromosome

instability, aneuploidy formation, and even cell death. SAC can ensure healthy cell growth and precise division. TTK is the core component of the spindle assembly checkpoint (SAC), and the function of SAC depends on the activity of TTK (35–37). Because TTK plays a vital role in maintaining chromosome stability, more and more researchers have begun to pay attention to the relationship between TTK expression and tumor development. Although TTK has conducted relevant basic and clinical studies in many human malignant tumors, we have not found similar studies in ovarian cancer. This study found that the expression level of TTK in tumor tissues was significantly elevated, while the expression in normal ovarian tissues was negative. It is confirmed with the existing literature that through Northern blot analysis, except for the testis and placenta, the TTK gene transcript is almost not detected in normal organs. However, high levels of TTK are easily found in many types of human malignancies, and the abnormal expression of TTK will inevitably affect the function of SAC (38). Compared with the same period last year, TTK is overexpressed in many malignant tumors, and the prognosis of patients with TTK overexpression is poor. We speculate that TTK may play a subtle role in the occurrence of ovarian cancer. It has been widely recognized that chromosomal instability is related to tumor heterogeneity, chromosomal abnormalities, and aneuploidy formation. the existence of aneuploidy can be found in the earliest stage of tumor formation, and chromosomal instability Stability is the basic process of tumorigenesis (39). At present, in gastric cancer and colorectal cancer with microsatellite instability, tumor-related TTK box shift mutations have been found, which can lead to the premature termination of TTK synthesis (40). Whether there is a similar process in ovarian cancer remains to be studied.

In addition to the difference in TTK expression in epithelial ovarian tumors and normal ovarian tissues, we further analyzed the TTK expression level in EOC patient tissues and its correlation with clinicopathological factors through the Chi-square test and found that TTK expression is related to tumor differentiation, There is a significant positive correlation between clinical stages. High TTK expression may contribute to tumor invasion, lymph node metastasis, and distant metastasis. For patients with the same clinical stage, the survival time of patients with low TTK expression is likely to be longer than that of patients with low TTK expression. The expression level of TTK can predict the development and outcome of EOC patients, and TTK can be used as a biomarker to predict the prognosis of EOC. To make some medical decisions for clinicians. For example, compared with patients with high TTK expression, ovarian cancer patients with low TTK expression are more likely to benefit from adjuvant chemotherapy. Clinically, for patients with early-stage ovarian cancer, if high TTK expression is found in these specimens, doctors and patients need to pay more attention, because these patients are potentially high-risk groups of lymphatic metastasis or distant metastasis in the future. Using a combination of conventional pathology and TTK expression may improve the survival prognosis of these patients.

It is worth mentioning that our research can provide a theoretical basis for TTK immunotherapy and targeted therapy in different tumors. TTK can be used as an ideal immune epitope antigen to induce strong peptide-specific cytotoxic T lymphocyte activity, thereby fighting tumor cells. Its safety, immunogenicity, and clinical reactivity have been confirmed in clinical trials including lung cancer, esophageal cancer, and cholangiocarcinoma (41–47). Even, TTK can be used as a new therapeutic target and become a new method for the treatment of some tumors, including glioblastoma, breast cancer,

hepatocellular carcinoma, lung cancer, and pancreatic cancer (48–52). And in the studies of glioblastoma, breast cancer, and lung cancer (53–55), it was found that the combination of TTK inhibitors and chemotherapeutics can improve the efficacy of chemotherapeutics and reduce the adverse reactions of chemotherapeutics. From many studies, we have found that TTK inhibits The agent can not only weaken the invasion and activity of tumor cells, increase autophagy and apoptosis, but also can combine with chemotherapy drugs to enhance the efficacy. For the above-mentioned tumors, TTK overexpression is fully utilized, TTK targeted therapy or immunotherapy is feasible, and whether TTK inhibitors can become a new EOC therapeutic target is still further confirmed.

Ovarian cancer is one of the most common malignant tumors of the female reproductive system. Its early clinical features are not significant and it is highly concealed. Therefore, most patients are difficult to detect and diagnose and treat in time. When the clinical diagnosis is made, the patient is already in the middle and advanced stages. It is not ideal, so improving the diagnostic accuracy of ovarian cancer has important clinical value and significance (56). Tumor markers, or tumor markers, are substances that are characteristically present in malignant tumor cells, or are abnormally expressed and secreted by them, or are abnormal substances produced by tumor cells to stimulate host-related cells, which reflect the occurrence and development of malignant tumors. A class of abnormal substances is used to evaluate the treatment and prognosis of malignant tumors. Tumor markers can exist in tumor tissues, blood, milk, bile, and other body fluids and excrements such as urine and feces of tumor patients (57). Therefore, the detection of relevant tumor markers by immunological, biological, or chemical methods can not only assess The severity of the disease and the prognostic outcome of treatment for patients with malignant tumors, and the detection of relevant representative markers for suspected patients also helps to improve the accuracy of existing examination techniques for the diagnosis of malignant tumors (58).

So far, effective methods for early detection of ovarian cancer are still lacking. In order to improve the prognosis and improve the quality of life of patients, the early diagnosis of ovarian cancer has always attracted people's attention. The traditional tumor marker CA125 is widely used in the diagnosis, treatment, and monitoring of ovarian cancer. High sensitivity, but easily affected by physiological factors such as menstruation. In comparison, HE4 has strong specificity in the diagnosis of ovarian cancer, but it also has certain limitations. Therefore, the joint measurement of multiple indicators

Materials And Methods

gene expression profiling data. GENE EXPRESSION OMNIBUS (GEO) is a public repository created by the National Center for Biotechnology Information (NCBI) to store various forms of high-throughput genomics data (14). Gene expression profile data (GSE54388, GSE27651, GSE18520, GSE26712) are all from the Gene Expression Database (GEO). The above data sets all contain gene expression profiles and contain at least 20 cancer and healthy control samples, which have also been used to publish related literature(15–19).

*comprehensive analysis of microarray data set.*Based on the programming language R, there are hundreds of software packages in Bioconductor for high-throughput sequencing in analytical genomics (20). Use hgu133plus2.db annotation package (version 3.2.3) and hgu133a.DB annotation package (version 3.2.3) to convert probe ID to gene name. The limma software package (version 3.40.2) (21) was used to normalize and log 2 conversions of the data in the data set, and the DEG of the ovarian cancer tissues in the 4 data sets compared with the control was identified through a linear model. $|\log_{2}FC| > 1.5$ and $P < 0.05$ were considered statistically significant for DEG. $|\log_{2}FC| > 1.5$ is considered to increase DEG, $|\log_{2}FC| < 1.5$ is considered to decrease DEG. The Venn-diagram software package (version 1.6.20) (22) is used to integrate the genes that meet the criteria in the four data sets and visualize them with a Venn diagram.

*functional and pathway enrichment analysis.*The Clusterprofiler package (version 3.10.2) was used to perform function and pathway enrichment analysis on DEGs to explore the biological significance, and the significance threshold was set at $P < 0.05$. Gene ontology (GO) function enrichment mainly describes the functions of genes and gene products in all organisms from three aspects: cell components (CC), biological processes (BP), and molecular functions (MF) (23). The Kyoto Encyclopedia of Genes and Genomes (KEGG) pathway enrichment analysis explains genes from their biochemical pathways and regulatory pathways (24).

*PPI network construction and module screening.*To evaluate the functional interaction of DEG, use the gene database STRING to search for protein interactions to map DEGS to the PPI network to generate a combined score, and the cut-off value is a comprehensive score \geq of 0.4. Cytoscape software (version 3.7.2) (25) was used to construct a PPI network for visualization and biological analysis to identify the interaction between DEG-encoded proteins in ovarian cancer. To improve sensitivity and specificity, we used Cytoscape plug-in Cytohubba's MCC algorithm (26) to perform the next biological analysis on 20 hub genes. At the same time, the Cytoscape plug-in Molecular Complex Detection (MCODE) is used to detect dense areas of the PPI network (Degree Cutoff = 2, Node Score Cutoff = 0.2, and K-Core = 2, maximum depth = 100 is set as an advanced option) (27), Select the module that meets both the MCODE score > 3 and the number of nodes > 4 and performs KEGG enrichment analysis on DEGs.

*survival analysis of central genes.*Kaplan-Meier Plotter is an online database containing a large number of gene expression data and clinical data of patients with ovarian cancer (28). We use this library to analyze the selected 20 hub genes to evaluate their prognostic value. The graph can directly display the log-rank P-value and the hazard ratio (HR) of the 95% confidence interval, and select genes with a log-rank P-value of < 0.05 .

*analysis of hub gene expression level .*In order to verify the expression of the hub gene in ovarian cancer, use GEPIA (gene expression profile interactive analysis) (29) to match the normal data of TCGA (tumor genome atlas) and GTEX (genotype tissue expression) to the selected hub genes that affect the prognosis, Setting $P < 0.01$ has significant statistical significance, and the level of gene expression is displayed in the form of box plots.

patient and paraffin-embedded tissue samples. This study was approved by the Ethics Committee of the Affiliated People's Hospital of Shanxi Medical University. From 2015 to 2020, the Department of Obstetrics and Gynecology, Affiliated People's Hospital of Shanxi Medical University collected 150 patients and postoperative paraffin-embedded specimens. The pathological diagnosis of all tissue sections was confirmed by internal experts, as follows: malignant group n = 93, borderline group n = 27, benign group n = 15, normal group n = 15. The pathological types of ovarian cancer are 65 cases of serous adenocarcinoma, 13 cases of mucinous adenocarcinoma, 10 cases of endometrioid carcinoma, and 5 cases of clear cell carcinoma. In the malignant group, there were 40 cases, 53 cases of well-differentiated and poorly differentiated. According to the standards of the International Federation of Obstetrics and Gynecology (FIGO, 2009), the pathological stage is judged as follows: FIGO I-II stage (36 cases) and FIGO III-IV stage (57 cases). Lymph node metastasis was judged as follows: no metastasis (48 cases), metastasis (55 cases). All patients were primary ovarian cancer, with complete clinical and pathological data. Patients who received chemotherapy, radiotherapy, and hormone therapy before surgery were not implemented in this study.(Table 1)

TTK immunohistochemistry and H score. All fresh tissue specimens were collected immediately after surgical resection and immersed in 10% neutral buffered formalin solution, and then embedded in paraffin. The paraffin-embedded tissue sections were 5 meters in thickness and stained by immunohistochemistry. Immunohistochemical staining is performed manually, and each slide is processed strictly in accordance with the immunohistochemistry protocol. TTK polyclonal antibody (ab219068, Abcam, UK, 1:100). Paraffin-embedded tissue sections were deparaffinized with xylene and gradient alcohol, washed with PBS, hot antigen retrieval, 3% hydrogen peroxide to block endogenous peroxides, and incubated with rabbit TTK antibody (1:500) at 4°C overnight. The reaction enhancement solution was added dropwise for 30 minutes, and then the enzyme-labeled anti-rabbit secondary antibody reagent was incubated for 30 minutes. Diaminobenzidine was used for color development, hematoxylin counterstaining, dehydration, and neutral resin mounting. The manufacturer recommends testicular tissue as a positive control. The immunohistochemical sections were independently evaluated blindly by two experienced pathologists. TTK staining is evaluated using the H scoring system, which is calculated by multiplying the total staining intensity by the percentage of positive cells (30–33). The staining intensity was graded from 0 to 3 (0 = negative, 1 = weak, 2 = medium, 3 = strong), and the percentage of positives increased from 0 to 100. In theory, the final high score is obtained in the range of 0 to 300.

Statistical analysis

Analyze the data with SPSS 26.0 statistical software, and perform a single factor chi-square test for the clinicopathological factors of epithelial ovarian cancer, the test level is $\alpha = 0.05$; the combined predictor can be obtained by logistic regression model analysis, and the predictive evaluation value of the research factors can be passed Receiver operating characteristic curve (ROC curve) for analysis, $\alpha = 0.05$.

Declarations

Thanks

Not applicable

Acknowledgements

Not applicable.

Funding

No funding was received

Availability of data and materials

The datasets analyzed during the current study are available in the GEO repository,

<https://www.ncbi.nlm.nih.gov/geo/query/acc.cgi?acc=GSE54388>

<https://www.ncbi.nlm.nih.gov/geo/query/acc.cgi?acc=GSE27651>

<https://www.ncbi.nlm.nih.gov/geo/query/acc.cgi?acc=GSE18520>

<https://www.ncbi.nlm.nih.gov/geo/query/acc.cgi?acc=GSE26712>.

Authors' contributions

QF designed the study. JB, QQ and HM analyzed and interpreted the microarray datasets, and produced the manuscript. JB wrote the paper and submitted the manuscript. JB and MM performed the experiments. All authors read and approved the final manuscript.

Ethics approval and consent to participate

This study has been approved by research ethics Shanxi Provincial People's Hospital Committee. Written notice Agree to conduct analysis of tissue specimens in this study

Obtained from the patient.

Patient consent for publication

Not applicable.

Competing interests

The authors declare that they have no competing interests.

References

1. Silvia T, Michele-Antonio C, Stefano M, Giorgio A, Palma M and Antonio R. Gynecological cancer among adolescents and young adults (AYA). *Ann Transl Med* 8:397, 2020

2. Moufarrij S, Dandapani A, Arthofer E, Gomez S, Srivastava A, Lopez-Acevedo M, Villagra A and Chiappinelli KB. Epigenetic therapy for ovarian cancer: promise and progress. *Clin Epigenet* 11:7, 2019.
3. Zeppernick F and Meinhold-Heerlein I. The new FIGO staging system for ovarian, fallopian tube, and primary peritoneal cancer. *Arch Gynecol Obstet* 290:839-842, 2014.
4. Schiavone MB, Herzog TJ, Lewin SN, Deutsch I, Sun XM, Burke WM and Wright JD. Natural history and outcome of mucinous carcinoma of the ovary. *Am J Obstet Gynecol* 205:480e1-480e8, 2011.
5. Charkhchi P, Cybulski C, Gronwald J, Wong FO, Narod SA and Akbari MR. CA125 and ovarian cancer: a comprehensive review. *Cancers* 12:3730, 2020.
6. Gong M, Yan CS, Jiang Y, Meng HY, Feng MM and Cheng WJ. Genome-wide bioinformatics analysis reveals CTCFL is upregulated in high-grade epithelial ovarian cancer. *Oncol Lett* 18:4030-4039, 2019.
7. Stewart C, Ralyea C and Lockwood S. Ovarian cancer: An integrated review. *Semin Oncol Nurs* 35:151-156, 2019.
8. Potenza E, Parpinel G, Laudani ME, Macchi C, Fuso L and Zola P. Prognostic and predictive value of combined HE4 and CA125 biomarkers during chemotherapy in patients with epithelial ovarian cancer. *Int J Biol Markers* 35:20-27, 2020.
9. Fisk HA, Mattison CP and Winey M. A field guide to the Mps1 family of protein kinases. *Cell Cycle* 3:439-442, 2004.
10. Sacristan C and Kops GJPL. Joined at the hip: kinetochores, microtubules, and spindle assembly checkpoint signaling. *Trends Cell Biol* 25:21-28, 2015.
11. Santaguida S and Amon. Short- and long-term effects of chromosome mis-segregation and aneuploidy. *Nat Rev Mol Cell Biol* 16:473-485, 2015.
12. Stratford JK, Yan F, Hill RA, Major MB, Graves LM, Der CJ and Yeh JJ. Genetic and pharmacological inhibition of TTK impairs pancreatic cancer cell line growth by inducing lethal chromosomal instability. *PLoS One* 12:e0174863-e0174863, 2017.
13. Riggs JR, Nagy M, Elsner J, Erdman P, Cashion D, Robinson D, Harris R, Huang D, Tehrani L, Deyanat-Yazdi G, *et al*. The discovery of a dual TTK protein kinase/CDC2-like kinase (CLK2) inhibitor for the treatment of triple negative breast cancer initiated from a phenotypic screen. *J Med Chem* 60:8989-9002, 2017.
14. King JL, Zhang B, Li Y, Li KP, Ni JJ, Saavedra HI and Dong JT. TTK promotes mesenchymal signaling via multiple mechanisms in triple negative breast cancer. *Oncogenesis* 7:69, 2018.
15. Yeung TL, Leung CS, Wong KK, Gutierrez-Hartmann A, Kwong J, Gershenson DM, and Mok SC. ELF3 is a negative regulator of epithelial-mesenchymal transition in ovarian cancer cells. *Oncotarget* 8:14951-14963, 2017.
16. King ER, Tung CS, Tsang YT, Zu Z, Lok GT, Deavers MT, Malpica A, Wolf JK, Lu KH, Birrer MJ, *et al*. The anterior gradient homolog 3 (AGR3) gene is associated with differentiation and survival in ovarian cancer. *Am J Surg Pathol* 35:904-912, 2011.

17. Mok SC, Bonome T, Vathipadiekal V, Bell A, Johnson ME, Wong KK, Park DC, Hao K, Yip DK, Donninger H, *at a* A gene signature predictive for outcome in advanced ovarian cancer identifies a survival factor: microfibril-associated glycoprotein 2 *Cancer Cell* 16 521-532, 2009.
18. Bonome T, Levine DA, Shih J, Randonovich M, Pise-Masison CA, Bogomolnii F, Ozbun L, Brady J, Barrett JC, Boyd J, *at a* A gene signature predicting for survival in suboptimally debulked patients with ovarian cancer *Cancer Res* 68 5478-5486, 2008
19. Vathipadiekal V, Wang V, Wei W, Waldron L, Drapkin R, Gillette M, Skates S and Birrer M Creation of a Human Secretome: A Novel Composite Library of Human Secreted Proteins: Validation Using Ovarian Cancer Gene Expression Data and a Virtual Secretome Array. *Clin Cancer Res* 21 4960-4960, 2015
20. Chen X, Yu C, Gao J, Zhu H, Cui B, Zhang T, Zhou Y, Liu Q, He H, Xiao R, *at a* A novel USP9X substrate TTK contributes to tumorigenesis in non-small-cell lung cancer *Theranostics* 8 2348-2360, 2018
21. Miao R, Wu Y, Zhang H, Zhou H, Sun X, Csizmadia E, He L, Zhao Y, Jiang C, Miksad RA, *at a* Utility of the dual-specificity protein kinase TTK as a therapeutic target for intrahepatic spread of liver cancer *Sci Rep* 6 33121, 2016
22. Tannous BA, Kerami M, Van der Stoop PM, Kwiatkowski N, Wang J, Zhou W, Kessler AF, Lewandrowski G, Hiddingh L, Sol N, *at a* Effects of the selective MPS1 inhibitor MPS1-IN-3 on glioblastoma sensitivity to antimitotic drugs *J Natl Cancer Inst* 105 1322-1331, 2013
23. Ling Y, Zhang X, Bai Y, Li P, Wei C, Song T, Zheng Z, Guan K, Zhang Y, Zhang B, *at a* Overexpression of Mps1 in colon cancer cells attenuates the spindle assembly checkpoint and increases aneuploidy *Biochem Biophys Res Commun* 450 1690-1695, 2014
24. Xie Y, Lin JZ, Wang AQ, Xu WY, Long JY, Luo YF, Shi J, Liang ZY, Sang XT and Zhao HT Threonine and tyrosine kinase may serve as a prognostic biomarker for gallbladder cancer *World J Gastroenterol* 23 5787-5797, 2017
25. Barrett T, Wilhite SE, Ledoux P, Evangelista C, Kim IF, Tomashevsky M, Marshall KA, Phillippy KH, Sherman PM, Holko M, *at a* NCBI GEO archive for functional genomics data sets—update *Nucleic Acids Research* 41 D991-D995, 2013
26. Huber W, Carey VJ, Gentleman R, Anders S, Carlson M, Carvalho BS, Bravo HC, Davis S, Gatto L, Girke T, *at a* Orchestrating high-throughput genomic analysis with Bioconductor *Nat Methods* 12 115-121, 2015
27. Ritchie ME, Phipson B, Wu D, Hu YF, Law CW, Shi W and Smyth GK Limma powers differential expression analyses for RNA-sequencing and microarray studies *Nucleic Acids Res* 43 e47, 2015
28. Chen HB and Boutros PC VennDiagram a package for the generation of highly-customizable venn and euler diagrams in R *BMC Bioinformatics* 12 35, 2011
29. Thomas PD The gene ontology and the meaning of biological function *Methods Mol Biol* 1446 15-24, 2017
30. Ogata H, Goto S, Sato K, Fujibuchi W, Bono H and Kanehisa M KEGG kyoto encyclopedia of genes and genomes *Nucleic Acids Res* 27 29-34, 1999

31. Kohl M, Wiese S and Warscheid B Cytoscape Software for visualization and analysis of biological networks Methods Mol Biol 696 291-303, 2011
32. Chin CH, Chen SH, Wu HH, Ho CW, Ko MT and Lin CY CytoHubba identifying hub objects and sub-networks from complex interactome BMC Syst Biol 8 S11, 2014
33. Bader GD and Hogue CWV An automated method for finding molecular complexes in large protein interaction networks BMC Bioinformatics 4 2, 2003
34. Gyorffy B, Lánczky A and Szállási Z Implementing an online tool for genome-wide validation of survival-associated biomarkers in ovarian-cancer using microarray data from 1287 patients Endocr Relat Cancer 19 197-208, 2012
35. Tang ZF, Li CW, Kang BX, Gao G, Li C and Zhang ZM GEPIA a web server for cancer and normal gene expression profiling and interactive analyses Nucleic Acids Res 45 W98-W102, 2017
36. Yeo W, Chan SL, Mo FKF, Chu CM, Hui JWY, Tong JHM, Chan AWH, Koh J, Hui EP, Loong H, *et al* Phase I/II study of temsirolimus for patients with unresectable hepatocellular carcinoma (HCC)- a correlative study to explore potential biomarkers for response BMC Cancer 15 395, 2015
37. Specht E, Kaemmerer D, Sanger J, Wirtz RM, Schulz S and Lupp A Comparison of immunoreactive score, HER2/neu score and H score for the immunohistochemical evaluation of somatostatin receptors in bronchopulmonary neuroendocrine neoplasms Histopathology 67 368-377, 2015
38. Liang PI, Li CF, Chen LT, Sun DP, Chen TJ, Hsing CH, Hsu HP and Lin CY BCL6 overexpression is associated with decreased p19 ARF expression and confers an independent prognosticator in gallbladder carcinoma Tumour Biol 35 1417-1426, 2014
39. Budwit-Novotny DA, McCarty KS, Cox EB, Soper JT, Mutch DG, Creasman WT, Flowers JL and McCarty KS Immunohistochemical analyses of estrogen receptor in endometrial adenocarcinoma using a monoclonal antibody Cancer Res 46 5419-5425, 1986
40. Kusakabe K, Ide N, Daigo Y, Itoh T, Yamamoto T, Hashizume H, Nozu K, Yoshida H, Tadano G, Tagashira S, *et al* Discovery of imidazo[1, 2-b]pyridazine derivatives selective and orally available Mps1 (TTK) kinase inhibitors exhibiting remarkable antiproliferative activity J Med Chem 58 1760-1775, 2015
41. Lauze E, Stoelcker B, Luca FC, Weiss E, Schutz AR and Winey M Yeast spindle pole body duplication gene MPS1 encodes an essential dual specificity protein kinase EMBO J 14 1655-1663, 1995
42. Lara-Gonzalez P, Westhorpe FG and Taylor SS The spindle assembly checkpoint Curr Biol 22 R966-R980, 2012
43. Musacchio A Spindle assembly checkpoint the third decade Philos Trans R Soc Lond B Biol Sci 366 3595-3604, 2011
44. Danielsen HE, Pradhan M and Novelli M Revisiting tumour aneuploidy the place of ploidy assessment in the molecular era Nat Rev Clin Oncol 13 291-304, 2016
45. Ahn CH, Kim YR, Kim SS, Yoo NJ and Lee SH Mutational analysis of TTK gene in gastric and colorectal cancers with microsatellite instability Cancer Res Treat 41 224-228, 2009

46. Suda T, Tsunoda T, Daigo Y, Nakamura Y and Tahara H Identification of human leukocyte antigen-A24-restricted epitope peptides derived from gene products upregulated in lung and esophageal cancers as novel targets for immunotherapy Cancer Sci 98 1803-1808, 2007
47. Suzuki H, Fukuhara M, Yamaura T, Mutoh S, Okabe N, Yaginuma H, Hasegawa T, Yonechi A, Osugi J, Hoshino M, *et al* Multiple therapeutic peptide vaccines consisting of combined novel cancer testis antigens and anti-angiogenic peptides for patients with non-small cell lung cancer J Transl Med 11 97, 2013
48. Mizukami Y, Kono K, Daigo Y, Takano A, Tsunoda T, Kawaguchi Y, Nakamura Y and Fujii H Detection of novel cancer-testis antigen-specific T-cell responses in TIL, regional lymph nodes, and PBL in patients with esophageal squamous cell carcinoma Cancer Sci 99 1448-1454, 2008
49. Kono K, Mizukami Y, Daigo Y, Takano A, Masuda K, Yoshida K, Tsunoda T, Kawaguchi Y, Nakamura Y and Fujii H Vaccination with multiple peptides derived from novel cancer-testis antigens can induce specific T-cell responses and clinical responses in advanced esophageal cancer Cancer Sci 100 1502-1509, 2009
50. Kono K, Inuma H, Akutsu Y, Tanaka H, Hayashi N, Uchikado Y, Noguchi T, Fujii H, Okinaka K, Fukushima R, *et al* Multicenter, phase II clinical trial of cancer vaccination for advanced esophageal cancer with three peptides derived from novel cancer-testis antigens J Transl Med 10 141, 2012
51. Inuma H, Fukushima R, Inaba T, Tamura J, Inoue T, Ogawa E, Horikawa M, Ikeda Y, Matsutani N, Takeda K, *et al* Phase I clinical study of multiple epitope peptide vaccine combined with chemoradiation therapy in esophageal cancer patients J Transl Med 12 84, 2014
52. Aruga A, Takeshita N, Kotera Y, Okuyama R, Matsushita N, Ohta T, Takeda K and Yamamoto M Long-term vaccination with multiple peptides derived from cancer-testis antigens can maintain a specific T-cell response and achieve disease stability in advanced biliary tract cancer Clin Cancer Res 19 2224-2231, 2013
53. Tannous BA, Kerami M, Van der Stoop PM, Kwiatkowski N, Wang J, Zhou W, Kessler AF, Lewandrowski G, Hiddingh L, Sol N, *et al* Effects of the selective MPS1 inhibitor MPS1-IN-3 on glioblastoma sensitivity to antimetabolic drugs J Natl Cancer Inst 105 1322-1331, 2013
54. Maia AR, de Man J, Boon U, Janssen A, Song JY, Omerzu M, Sterrenburg JG, Prinsen MB, Willemsen-Seegers N, de Roos JA, *et al* Inhibition of the spindle assembly checkpoint kinase TTK enhances the efficacy of docetaxel in a triple-negative breast cancer model Ann Oncol 26 2180-2192, 2015
55. Wu ZX, Yang Y, Wang G, Wang JQ, Teng QX, Sun L, Lei ZN, Lin L, Chen ZS and Zou C Dual TTK/CLK2 inhibitor, CC-671, selectively antagonizes ABCG2-mediated multidrug resistance in lung cancer cells Cancer Sci 111 2872-2882, 2020
56. Chang L, Ni J, Zhu Y, Pang B, Graham P, Zhang H and Li Y Liquid biopsy in ovarian cancer recent advances in circulating extracellular vesicle detection for early diagnosis and monitoring progression Theranostics 9 4130-4140, 2019
57. Zhang D, Jiang YX, Luo SJ, Zhou R, Jiang QX and Linghu H Serum CA125 levels predict outcome of interval debulking surgery after neoadjuvant chemotherapy in patients with advanced ovarian

cancer. Clin Chim Acta 484:32-35, 2018

58. Bonifácio VDB. Ovarian cancer biomarkers: moving forward in early detection. Adv Exp Med Biol 1:255-263, 2020

Tables

Table I Clinicopathological characteristics of the cohort

Characteristics	Cases
Age(years)	
≤52	38
>52	55
Clinical stages	
I-II	36
III-IV	57
Lymphatic metastasis	
with	48
without	45
ascites	
with	55
without	38
Histological differentiation	
Intermediately and well differentiated.	40
Poorly differentiated	53
Pathological type	
Serous	65
Non-serous	28
Whether to give birth	
with	76
without	17
Distant metastasis	
with	53
without	40
CA125≤ 35	
Normal	28
Elevated	65

HE4-140	
Normal	30
Elevated	63

Table II Details for GEO ovarian cancer data

Reference	GEO	PMID	Sample	Platform	Normal	Tumor
Yeung T et al.[15]	GSE54388	28199976	Ovary	GPL570 [HG-U133_Plus_2] Affymetrix Human Genome U133 Plus 2.0 Array	6	16
Wong K[16]	GSE27651	21451362	Ovary	GPL570 [HG-U133_Plus_2] Affymetrix Human Genome U133 Plus 2.0 Array	6	43
Birrer MJ[17]	GSE18520	19962670	Ovary	GPL570 [HG-U133_Plus_2] Affymetrix Human Genome U133 Plus 2.0 Array	10	53
Birrer MJ[18-19]	GSE26712	18593951 25944803	Ovary	GPL96 [HG-U133A] Affymetrix Human Genome U133A Array	10	185

Table III ALL 105 commonly DEGs were detected from four profile datasets,including 33 up-regulated genes and 102 down-regulated genes in the ovarian cancer tissues compared to normal ovary tissues.

DEGS	Genes Name
Up-regulated 33 genes	CRABP2 EPCAM TRIP13 CKS2 INAVA TTK MTHFD2 SOX17 PFKP RACGAP1 KLK6 CLDN3 CDC20 MMP7 SOX9 IDH2 CD24 UBE2C SCGB2A1 LYPD1 CP HIST1H1C DEFB1 S100A2 GLDC PRAME MAL IFI27 ISG15 CLDN10 LCN2 SST SCGB1D2
Down-regulated 102 genes	ABCA8 CALB2 DIRAS3 MAF PRG4 PDE8B GPRASP1 NPY1R REEP1 OGN SNCA CHGB TCF21 GNG11 ADH1B NDNF PTGIS GSDME LGALS2 SPOCK1 MTUS1 RNASE4 CLEC4M KDR TCEAL2 GFPT2 PCDH9 BNC1 C1S MNDA SFRP1 IGFBP6 PROCR HSD17B2 NELL2 GPM6A SNCAIP HBB OLFML1 CELF2 ALDH1A1 ATP10D RNF128 BAMBI CMAHP PEG3 MST1 PDPN HAS1 AKT3 PTPRZ1 CSGALNACT1 SLC31A2 PKD2 GHR FRY CHRDL1 NAP1L3 BCHE PDGFD TSPAN8 PDGFRA DSE CFH PCOLCE2 FGF13 WNT5A ALDH1A3 RGS4 PMP22 CAV1 TMEM255A MEOX2 RARRES1 PRKAR2B SEMA3C PROS1 FLRT3 PLSCR4 KLF4 GAS1 EFEMP1 SLC39A8 CADPS2 ARMCX1 NDN DPYD AQP9 NEFH LOC728392 MEIS2 LAMB1 ADAMTS3 ZFPM2 FGF9 MARCO STK26 SCG5 DSC3 HSPA2 CSTA TFPI2

Table IV Gene ontology analysis of DEGs in ovarian cancer

Expression	Category	Term	Description	Count	P-value	
up-regulated	GOTERM_BP_DIRECT	GO:0007094	mitotic spindle assembly checkpoint	3	2.034627E-05	
	GOTERM_BP_DIRECT	GO:0051983	regulation of chromosome segregation	4	2.190205E-05	
	GOTERM_BP_DIRECT	GO:1902099	regulation of metaphase/anaphase transition of cell cycle	3	7.461011E-05	
	GOTERM_BP_DIRECT	GO:1904668	positive regulation of ubiquitin protein ligase activity	2	2.017870E-04	
	GOTERM_BP_DIRECT	GO:0023019	signal transduction involved in regulation of gene expression	2	5.187441E-04	
	GOTERM_BP_DIRECT	GO:0007059	chromosome segregation	4	1.393029E-03	
	GOTERM_CC_DIRECT	GO:0005680	anaphase-promoting complex	2	5.851398E-04	
	GOTERM_CC_DIRECT	GO:0005923	bicellular tight junction	3	1.066608E-03	
	GOTERM_CC_DIRECT	GO:0070160	tight junction	3	1.202291E-03	
	GOTERM_CC_DIRECT	GO:0043296	apical junction complex	3	1.537972E-03	
	GOTERM_CC_DIRECT	GO:0000152	nuclear ubiquitin ligase complex	2	1.923558E-03	
	down-regulated	GOTERM_BP_DIRECT	GO:0001505	regulation of neurotransmitter levels	11	1.055171E-06
		GOTERM_BP_DIRECT	GO:0050818	regulation of coagulation	6	3.860156E-06
GOTERM_BP_DIRECT		GO:0060485	mesenchyme development	9	9.267618E-06	
GOTERM_BP_DIRECT		GO:0061437	renal system vasculature development	4	1.014772E-05	
GOTERM_BP_DIRECT		GO:0061440	kidney vasculature development	4	1.014772E-05	
GOTERM_BP_DIRECT		GO:0007596	blood coagulation	10	1.019607E-05	

GOTERM_CC_DIRECT	GO:0031012	extracellular matrix	13	1.132046E-06
GOTERM_CC_DIRECT	GO:0062023	collagen-containing extracellular matrix	10	5.076567E-05
GOTERM_CC_DIRECT	GO:0072562	blood microparticle	6	1.317312E-04
GOTERM_MF_DIRECT	GO:0008201	heparin binding	6	1.440927E-04
GOTERM_MF_DIRECT	GO:0005109	frizzled binding	3	2.134040E-04

Table V KEGG pathway analysis of genes in each module

	Pathway	ID	P-value	P-adjust	Count	Genes
Module 1	Cell cycle	hsa04110	0.001427147	0.005143403	2	TTK CDC20
	Ubiquitin mediated proteolysis	hsa04120	0.001714468	0.005143403	2	UBE2C CDC20
Module 2	NULL					
Module 3	Ferroptosis	hsa04216	0.010068528	0.042095249	1	CP
	Porphyrin and chlorophyll metabolism	hsa00860	0.010570617	0.042095249	1	CP
	ECM-receptor interaction	hsa04512	0.022083515	0.042095249	1	LAMB1
	Small cell lung cancer	hsa05222	0.023081453	0.042095249	1	LAMB1
	Amoebiasis	hsa05146	0.025574068	0.042095249	1	LAMB1
	Toxoplasmosis	hsa05145	0.028063499	0.042095249	1	LAMB1

Table VI TTK expression in epithelial ovarian tumors

parameters	n	TTK expression		χ^2	P-value	
		negative	positive			
normal	15	15 (100%)	0 (0%)		<0.001	
benign	15	8 (53.3%)	7 (46.7%)	68.09	<0.001	
Borderline	27	17 (63.0%)	10 (37.0%)	40.19	<0.001	
Malignant (control)	93	7 (7.5%)	86 (92.5%)	-	-	
cytoplasm	Proportion of positive cells (%)			Number of cases		
	Median (range)					
	malignant tumor	Borderline tumor	benign tumor	malignant tumor	Borderline tumor	benign tumor
negative	-	-	-	7	17	8
positive	90 (20-100)	55 (10-70)	30 (5-40)	86	10	7
1+	90 (70-100)	55 (10-70)	30 (5-40)	24	7	6
2+	90 (40-100)	30 (10-35)	30	40	3	1
3+	85 (70-100)	-	-	22	-	-

Table VII Correlations between TTK expressions and clinicopathological parameters

parameters	TTK expression		χ^2	P-value
	High expression	low expression		
Age(years)			0.498	0.480
	≤52	20[52.6%]	18[47.4%]	
	>52	28[60.0%]	27[40.0%]	
Clinical stages			13.362	<0.001
	I-II	10[27.8%]	26[72.2%]	
	III-IV	38[66.7%]	19[33.3%]	
Lymphatic metastasis			18.028	<0.001
	with	35[72.9%]	13[27.1%]	
	without	13[28.9%]	32[71.1%]	
ascites			24.029	<0.001
	with	40[72.7%]	15[27.3%]	
	without	8[21.1%]	30[78.9%]	
Histological differentiation			19.905	<0.001
	Intermediately and well differentiated	10[25.0%]	30[75.0%]	
	Poorly differentiated	38[71.7%]	15[28.3%]	
Pathological type			4.055	0.044
	Serous	38[58.5%]	27[41.5%]	
	Non-serous	10[35.7%]	18[64.3%]	
Whether to give birth			0.173	0.678
	with	40[52.6%]	36[47.4%]	
	without	8[47.1%]	9[52.9%]	
Distant metastasis			37.675	<0.001
	with	42[79.2%]	11[20.8%]	
	without	6[15.0%]	34[85.0%]	
CA125[0-35]			8.516	0.004

	Normal	8 (28.6%)	20 (71.4%)		
	Elevated	40 (61.5%)	25 (38.5%)		
HE4 (0-140)				5.925	0.015
	Normal	10 (33.3%)	20 (66.7%)		
	Elevated	38 (60.3%)	25 (39.7%)		

Table VIII Multivariate analysis of ovarian cancer

parameters	<i>b</i>	<i>S.E</i>	<i>Wald</i> χ^2	<i>P</i>	<i>OR</i>	<i>OR 95% of the CI</i>	
						upper limit	lower limit
Distant transfer (yes)	3.07	0.55	30.41	0.00	21.63	7.25	64.52
Lymph node metastasis (yes)	1.89	0.46	16.73	0.00	6.62	2.67	16.39
Clinical Phases (Phase I-II)	-1.64	0.46	12.50	0.00	0.19	0.07	0.48
degree of differentiation (Intermediately and well differentiated)	-2.02	0.47	18.17	0.00	0.13	0.052	0.33
CA125(Elevated)	1.38	0.49	8.00	0.005	4.00	1.53	10.49
HE4(Elevated)	1.11	0.46	5.71	0.17	3.04	1.22	7.56
Abdominal water (yes)	2.51	0.50	24.40	0.00	12.30	4.54	33.31

Figures

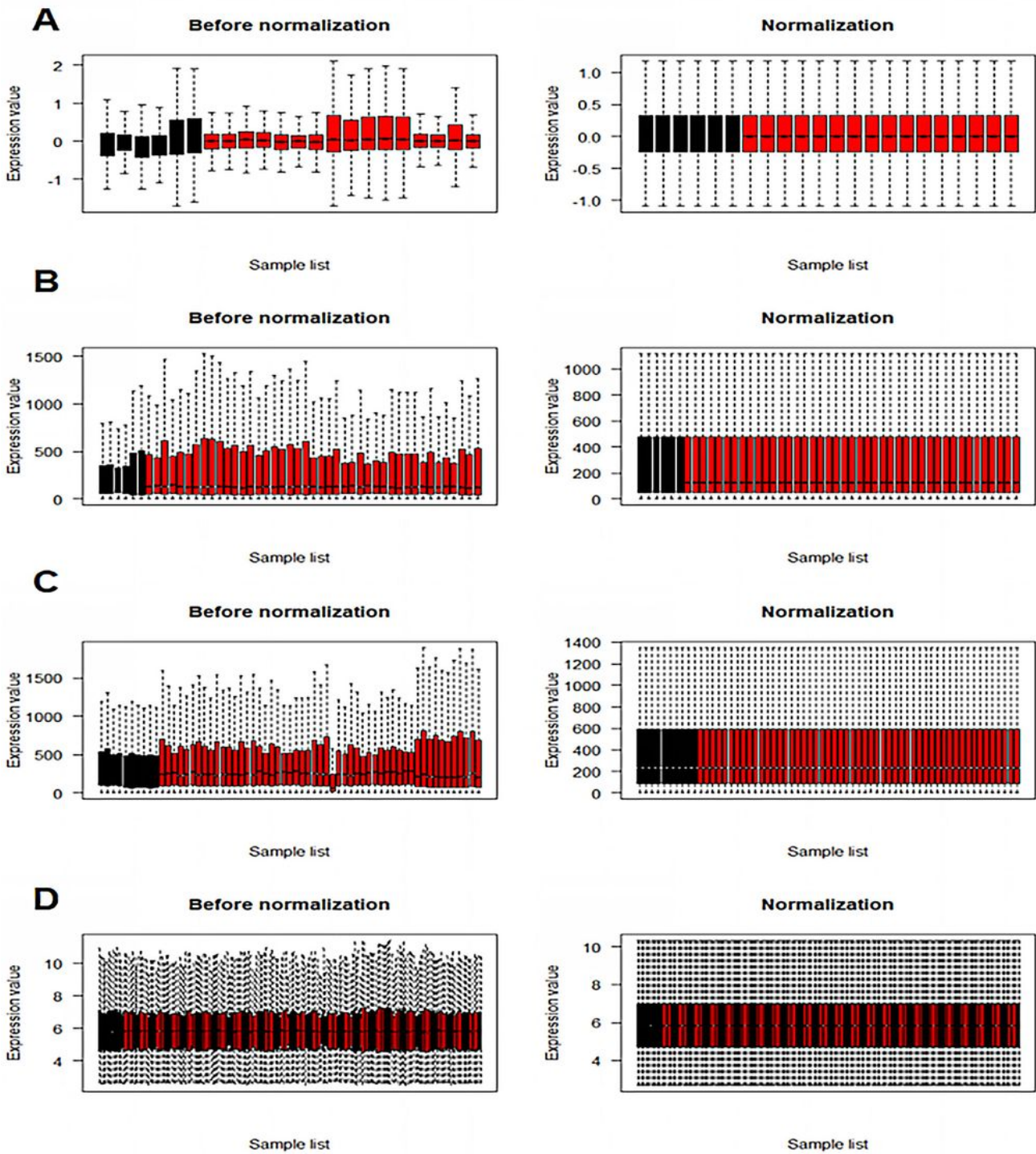


Figure 1

Standardization of gene expression. (A)The standardization of GSE54388 data,(B)the standardization of GSE27651 data,(C) the standardization of GSE18520 data,and(D)the standardization of GSE27651 data. The red bar represents the ovarian cancer samples expression value,and the black bar represents the healthy tissue samples expression value.

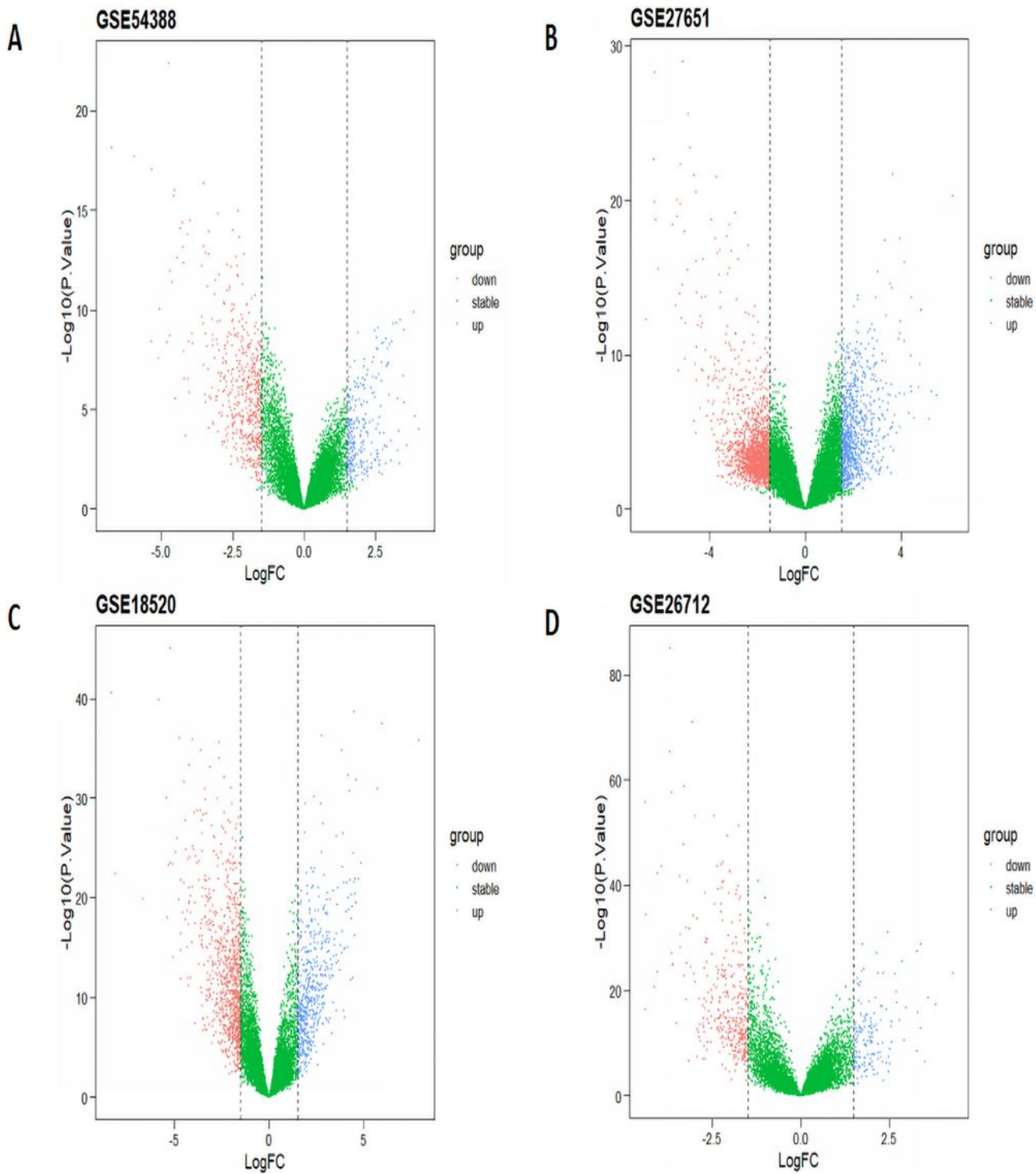


Figure 2

Volcano plot of gene expression profile data in ovarian cancer samples and normal ones.(A)Volcano plot of GSE54388,(B)Volcano plot of GSE27651,(C)Volcano plot of GSE18520,(D)Volcano plot of GSE26712.Blue plots represented lower expression levels genes with fold change ≥ 1.5 red plots represented higher expression levels genes with fold change ≤ 1.5 .Green plots represented the rest genes with no significant expression change.

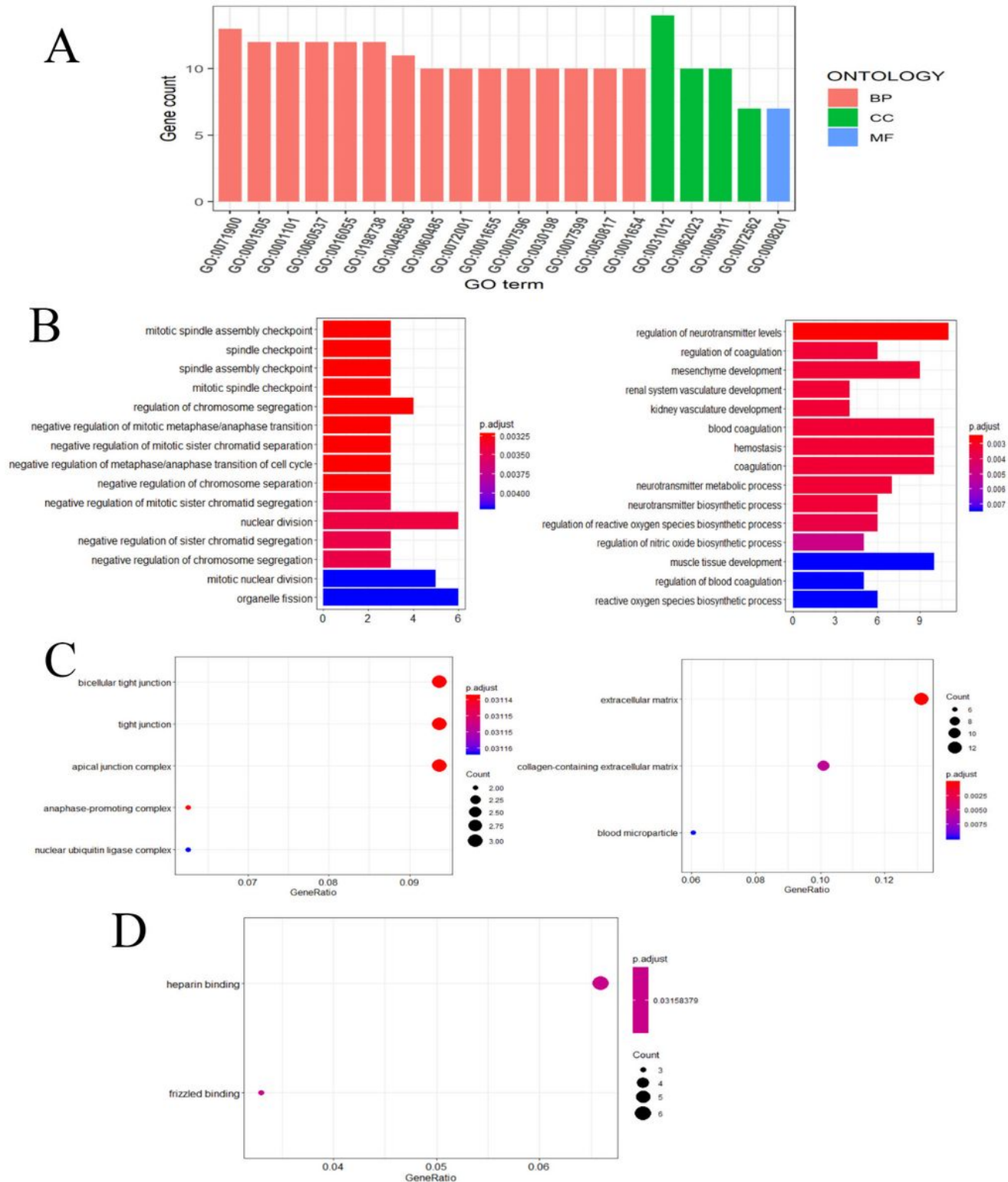


Figure 3

GO enrichment analysis of DEGs in ovarian cancer. (A) GO analysis divided DEGs into three functional groups:biological process (BP),cellular composition(CC)and molecular function(MF).(B)There are two barplots,the left side is the top15 of biological process of up-regulated DEGs,the right side is the top 15 of down-regulated DEGs.(C) There are two dotplots,the left side is the cellular composition of up-regulated

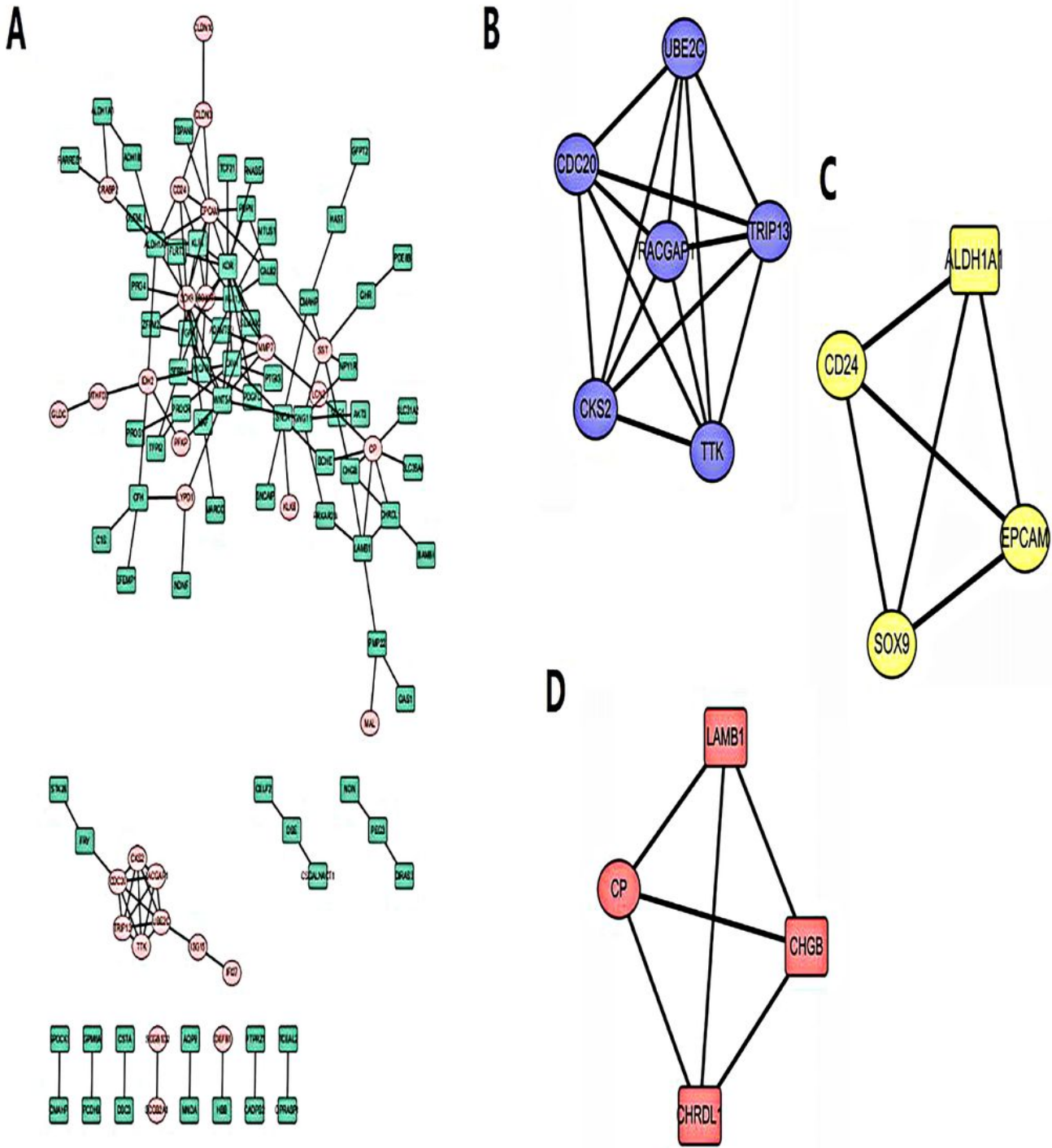


Figure 5

(A)PPI network with 106 DEGs.The nodes meant proteins,the edges meant the interaction of proteins;green rectangle meant down-regulated DEGs and pink circle meant up-regulated DEGs. Module analysis via Cytoscape software.(B)Module 1 : TRIP13-RACGAP1-CKS2-UBE2C-TTK-CDC20 (C)Module 2: ALDH1A1-CD24-EPCAM-SOX9 (D)Module 3: CP-LAMB1-CHRDL1-CHGB

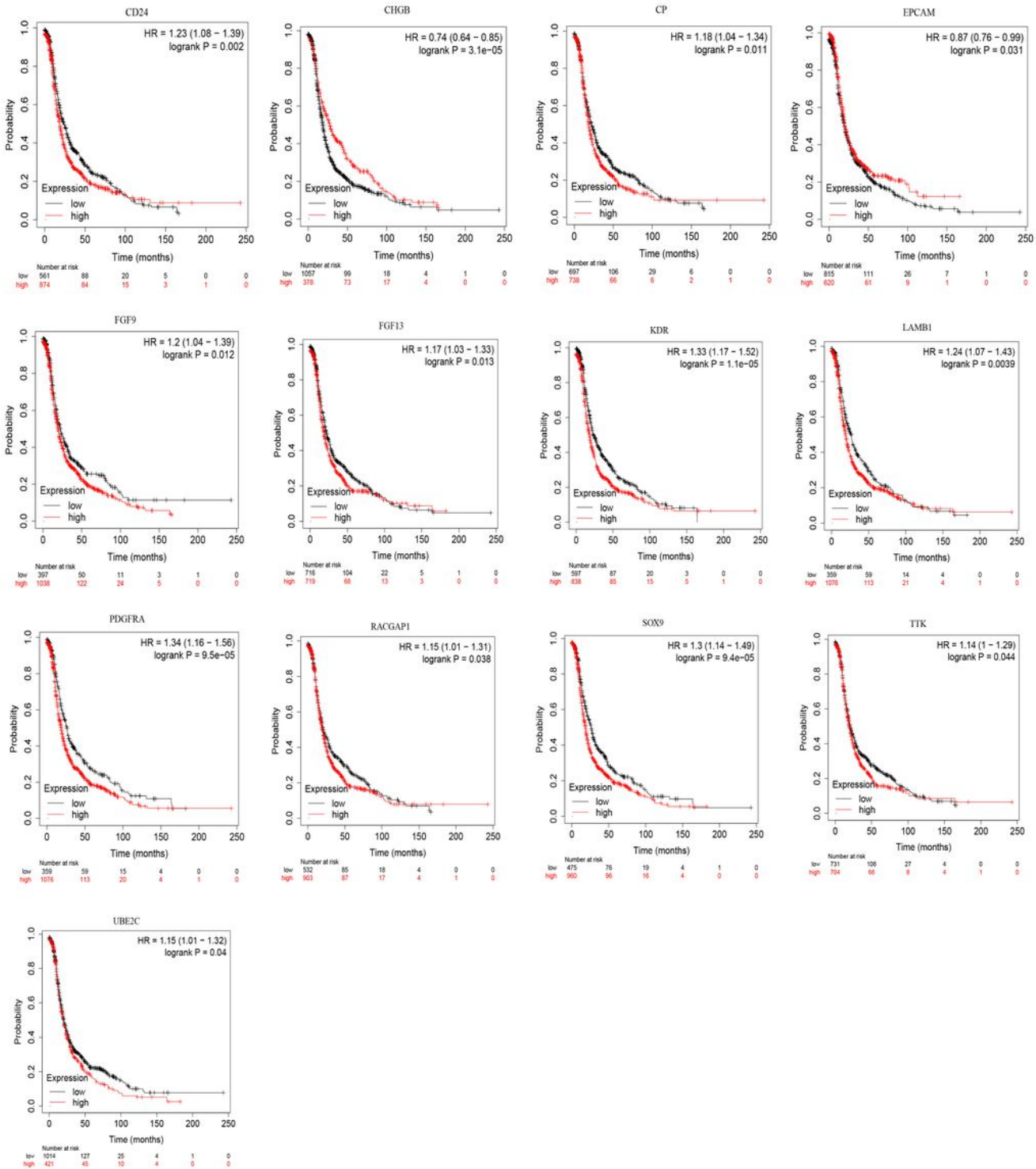


Figure 6

The prognosis of 20 hub genes was analyzed with Kaplan-Meier Plotter, and 13 genes had significantly poor survival rate ($P < 0.05$).

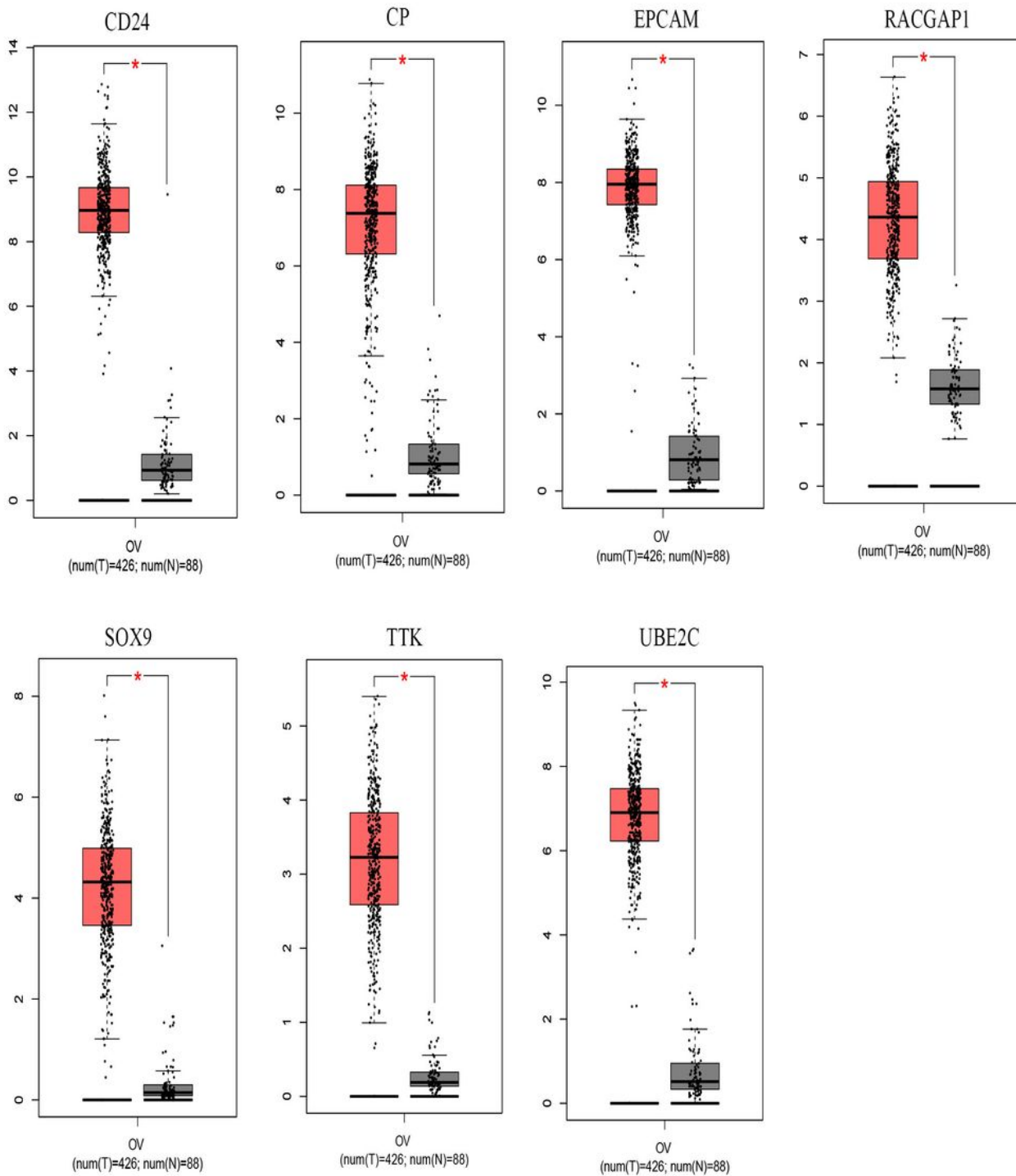


Figure 7

An analysis of gene expression levels on the GEPIA website found that 7 of 13 genes with poor prognosis were significantly expressed in ovarian cancer samples ($P < 0.01$). The red and grey boxes represent ovarian cancer and normal tissues respectively.

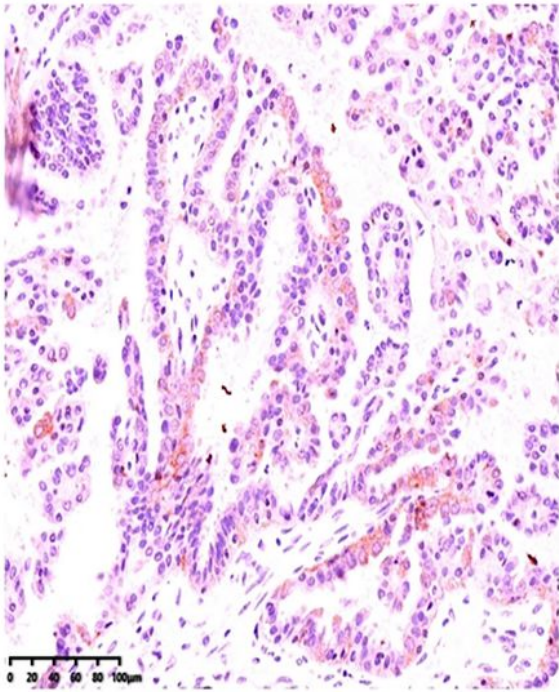
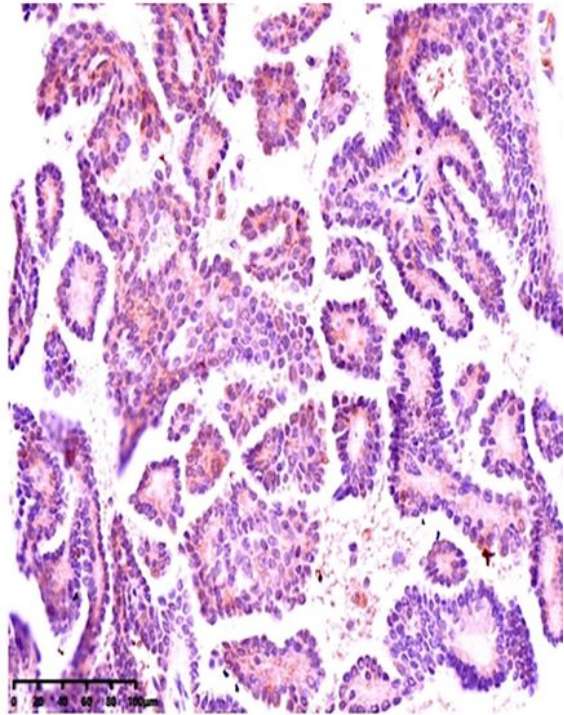
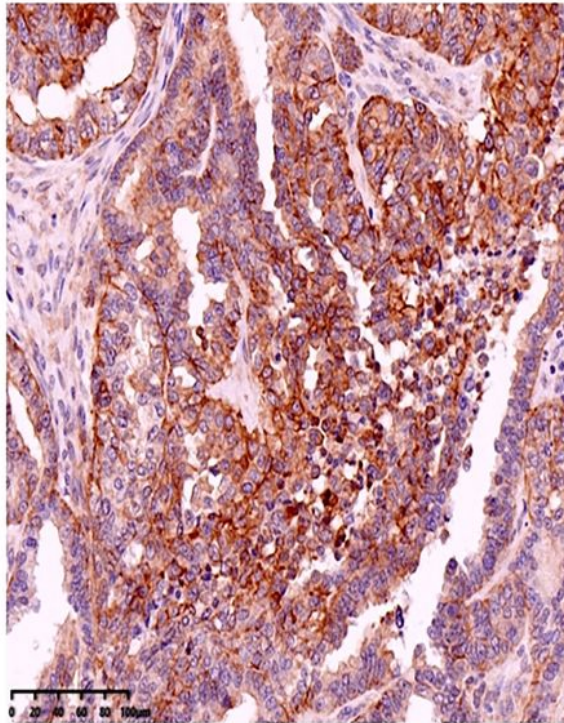
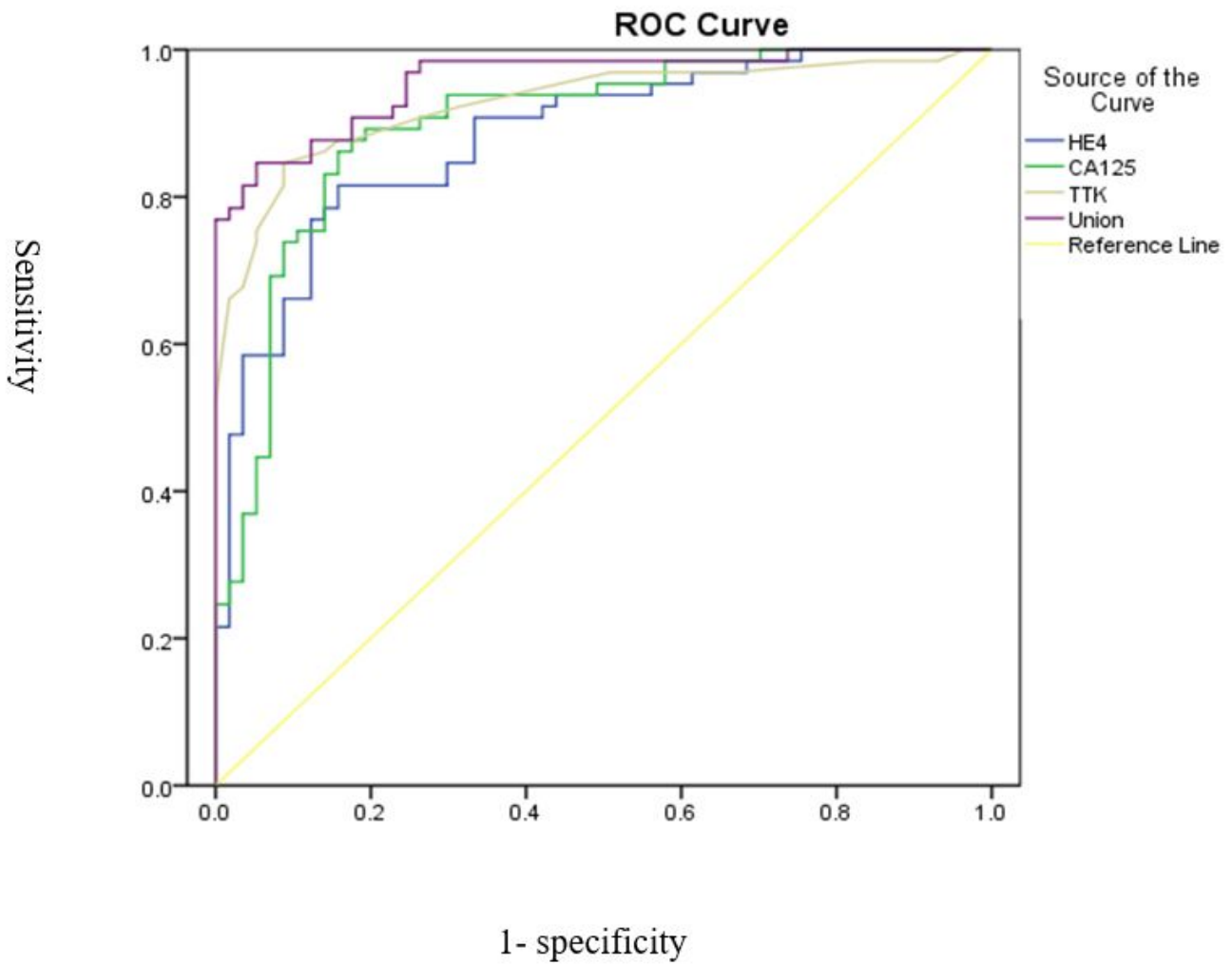
A**B****C**

Figure 8

cytoplasm staining with 1+ 2+ and 3+ intensity respectively



	HE4	CA125	TTK	Union
Area under the curve	0.882	0.899	0.927	0.958

Figure 9

ROC